REVIEW

Syn-shearing mobility of major elements in ductile shear zones: state of the art for felsic deformed protoliths

Fabrizio Tursi [1], Vincenzo Festa [1,*], Annamaria Fornelli [1], Francesca Micheletti [1], Richard Spiess [2]

[1] Department of Earth and Geo-environmental Sciences, University of Bari "Aldo Moro", via E. Orabona 4, 70125 Bari, Italy
[2] Department of Geosciences, University of Padova, via G. Gradenigo 6, 35131 Padova, Italy

ABSTRACT

The mineral assemblages of rocks, involved into ductile shear zones which act as open systems, may be strongly influenced by the occurrence of mass transfer processes induced by channeling H_2O-rich fluids and mobilizing major elements. In this respect, the mineralogy of ductilely sheared felsic rocks under metamorphic conditions is believed to be controlled mainly by the following variables: the infiltrated fluid fluxes, the thermobaric deformation conditions of felsic rocks, the tectonic context and the fluid source. To investigate the presence of common features regarding the gain and loss of mobilized major elements with respect to these variables, a review of literature case studies dealing with felsic sheared protoliths has been made.

Our findings suggest that: (i) the mobilization of preferred major elements seems not related to fixed values of time-integrated fluid flux; (ii) no general relations exist between the mobility of major elements and the tectonic context for shearing, with some exception; (iii) H_2O, K, Ca, Na, Mg, Si and Fe exhibit the greatest mobility whatever P-T metamorphic conditions; (iv) fluids coming from far-field and near-field sources induced preferred mobility of major elements within ductile shear zones; (v) the chemical selection of major elements seems greatly related to the fluid chemistry, while the amounts of fluids seems only to drive at completion the metamorphic fluid-rock reactions within ductile shear zones.

Keywords: ductile shear zones; felsic rocks; major element mobility; fluid-flux; fluid sources; fluid-rock interaction.

INTRODUCTION

A number of ductile shear zones are considered as preferential channels through which large quantities of H_2O-rich fluids interact at different thermobaric conditions and tectonic contexts with the strongly deforming rocks (Figure 1 a,b; e.g. Gasquet et al., 1981; Etheridge et al., 1983; McCaig, 1988; Selverstone et al., 1991; Wintsch et al., 1995; Pili et al., 1999; Rumble et al., 2003; Maggi et al., 2014). Mass transfer processes, governed by the channeling H_2O-rich fluids (e.g. Figure 1 a,b), profoundly modify the bulk rock chemistry of the deforming rocks (e.g. Figure 1b), so that the mobilization of major elements will control mineral reactions and the stability of mineral assemblages (e.g., Harlov and Austrheim, 2013, and references therein) together with the P-T conditions.

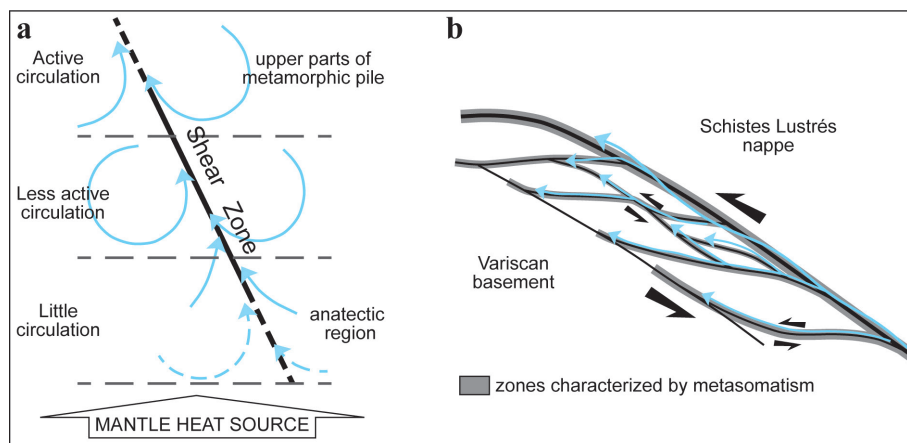Since over three decades great attention has been

Figure 1. Examples of H$_2$O-rich fluids (pale blue arrows) channeled within shear zones. a) Schematic model of fluid circulation in metamorphic belt (modified after Etheridge et al., 1983). b) Conceptual fluid-rock interaction model during deformation along the East Tenda Shear Zone (modified after Maggi et al., 2014).

paid to the mobility of major elements and hence to the change of the compositional space of ductile shear zones involving felsic protoliths. With the outstanding analysis of case studies regarding time-integrated fluid fluxes within ductile shear zones developed at amphibolite facies conditions, Dipple and Ferry (1992) contributed to a better understanding of fluid reservoirs involved during deformation. They concluded that extraction of fluids may occur from sources located close to ductile shear zones, i.e. from the host-hangingwall or -footwall, promoting major element mobility within them. Subsequently, several other case studies added new important insights on the potential location of fluid sources, confirming its shear zone near-field position (Bialek, 1999; van Staal et al., 2001; Sassier et al., 2006; Maggi et al., 2014) or showing that it can be located also in the far-field of shear zones (Selverstone et al., 1991; Demény et al., 1997; Hippertt, 1998; Streit and Cox, 1998; Cartwright and Buick, 1999; Oliot et al., 2010; Raimondo et al., 2011; Goncalves et al., 2012; Rossi and Rolland, 2014; Tsunogae and Van Reenen, 2014; Diener et al., 2016; Rolland and Rossi, 2016). Furthermore, these case studies, which concentrated on major element mobility in mylonitic felsic protoliths, provided also constraints on the P-T conditions and the tectonic context at which ductile shear zones developed. Although from the single case studies important insights regarding major element mobility in ductile shear zones arose, no attempt has been dedicated to the recognition of potential common features in terms of major element mobility within ductile shear zones. This attempt is the aim of the present review paper. For obtaining this goal, an extensive excursion through the literature data concerning major element mobility within ductile shear zones developed under metamorphic

conditions has been undertaken. Therefore, the present paper focuses on the most important variables potentially controlling the major element mobility in ductile shear zones (Tobisch et al., 1991), namely the infiltrated fluid fluxes, the thermobaric deformation conditions of felsic rocks, the tectonic context and the likely fluid source, being located in the host-rocks or in a far-field position of the ductile shear zone.

METHODS FOR ESTIMATING MAJOR ELEMENT MOBILITY AND FLUID-ROCK INTERACTION
Major element mobility
Different methods have been applied since 1967 to establish the mobility of chemical elements in ductile shear zones (e.g., Gresens, 1967; Grant, 1986; Baumgartner and Olsen, 1995).

Gresens (1967) first formulated an equation able to constrain the mobility of an element i in a natural system:

$$\Delta m_i = Fv \cdot m_i^a (\rho_a / \rho_0) - m_i^0 \qquad (1)$$

Where Δm_i is the amount of component i gained or lost, Fv is the volume factor expressing the ratio between the final and initial volume of the ductile shear zone, ρ_0 and ρ_a represent the original and modified rock densities, respectively, m_i^0 and m_i^a represent the weight percentages of the component i before and after the fluid-rock interaction event, respectively. Solving Equation (1), when $\Delta m_i = 0$ the element i is immobile; when $\Delta m_i > 0$ or $\Delta m_i < 0$, the element i is gained or lost, respectively. For ductile shear zones with no volume changes Fv is equal to 1. Based on this assumption, Gresens (1967) proposed an Fv vs Δm_i diagram with $Fv=1$ and $\Delta m_i = 0$ as reference frame to calculate the loss or gain of an element at
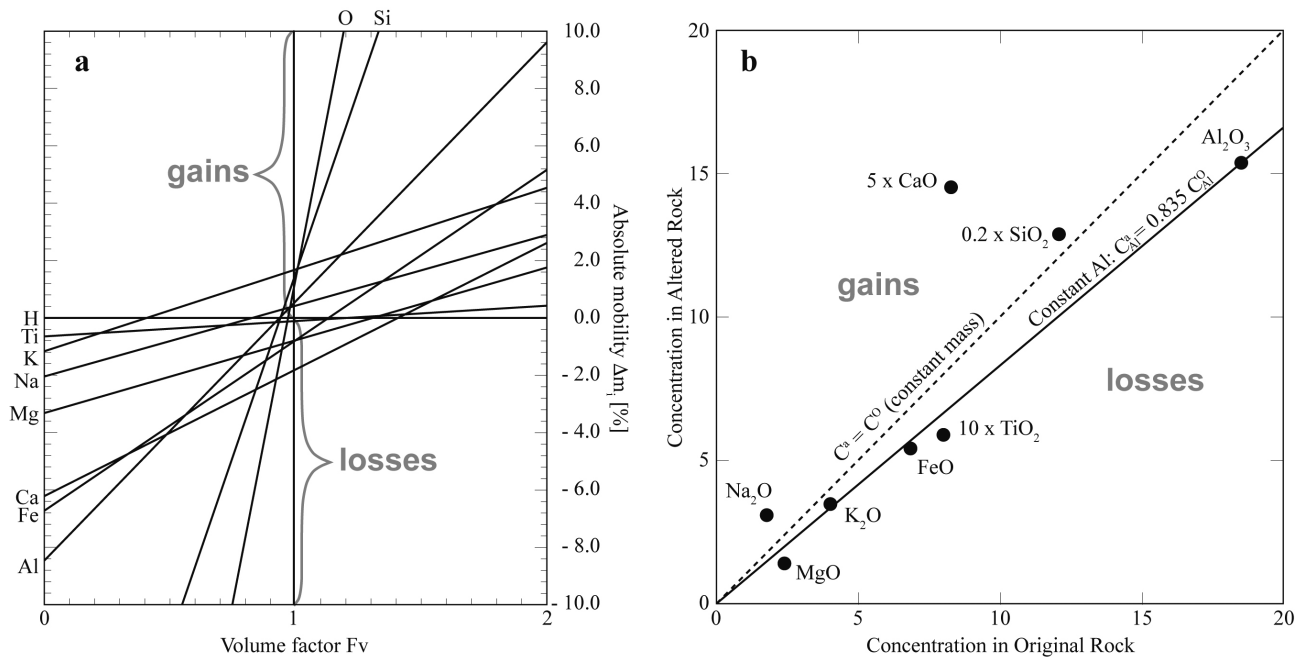
Figure 2. a) Absolute mobility of major elements Δm_i vs Fv Gresens (1967) diagram. With Δm_i, gain or loss of component i (in mass percentage of initial rock) and m_i^0 weight percentage of this constituent in initial rock (modified after Potdevin, 1993). b) Isocon diagram of Grant (1986). Some oxides have been scaled to provide a better distribution of data points (modified after Winter, 2014). Altered Rock means chemically modified rock.

constant volume conditions during fluid assisted element exchange (Figure 2a). For gains and losses, lines derived by the solution of Equation (1) for each element will intercept the Fv=1 line above or below the Δm_i=0 line, respectively. The line related to Al, which is usually considered an immobile element, intercepts the Δm_i=0 line at $Fv \approx 1$, supporting a substantially constant volume condition during fluid assisted mylonitization. If the fluid assisted mylonitization is associated to volume changes, with $Fv \neq 1$, immobile elements as e.g. Al, can be used as references for the calculation of the Fv value (Figure 2a). The plot of the Al line in Figure 2 is determined by solving the Equation (1) with Δm_i=0. The interception between the Al line and the Δm_i=0 line, in the Fv vs Δm_i diagram, represents the Fv estimation, which can be used for the solution of the Equation (1) related to the other elements. Therefore, for gains and losses, lines derived by solving Equation (1) for each element will intercept the $Fv \neq 1$ line above or below the Δm_i=0 line, respectively. Among the considered literature case studies, only Oliot et al. (2010) adopted this method, modified after Potdevin and Marquer (1987).

Grant (1986) rearranged the Equation (1) of Gresens (1967) and developed an alternative, simplified approach, proposing the following equation:

$$C_i^a = (m^0/m^a) \cdot (C_i^0 + \Delta C_i) \qquad (2)$$

where ΔC_i is the change in concentration of the element i, C_i^0 and C_i^a are the concentrations of the element i in the unaltered and the chemically modified rock, respectively, and m^0 and m^a are the mass of the rock before and after chemical modification, respectively.

Grant (1986) constructed a C_i^0 vs C_i^a diagram in which the ideal isocon line with a slope of 1.0 is obtained for $C_i^a = C_i^0$, therefore ΔC_i (i.e., $C^a = C^o$ in Figure 2b), and $m^a = m^o$ (Figure 2b). Thus, for gains and losses, the points related to the C_i^a and C_i^0 for each element will plot in the fields above or below the ideal isocon line, respectively. In real cases, where the rock involved in the fluid assisted exchange process experienced mass change, an immobile element, such as Al, is characterized by ΔC_i=0 and $m^a \neq m^o$. Therefore, the Al isocon, obtained by the solution of Equation (2), can be used as reference frame for the mobility of the other elements: the calculated C_i^a and C_i^0 for Al (i.e., C_{Al}^a and C_{Al}^0, respectively) plot on the proper Al-isocon (Figure 2b), whereas the points of elements affected by gains or losses show C_i^a and C_i^0 values that plot in the fields above or below the Al-isocon. In the considered case studies of the present paper, this approach was used by Selverstone et al. (1991), Demény et al. (1997), Hippertt (1998), Streit and Cox (1998), Bialek (1999), Cartwright and Buick (1999), Sassier et al. (2006), Raimondo et al. (2011), and Rolland and Rossi (2016).

To refine the approach of Grant (1986), Baumgartner and Olsen (1995) proposed an algorithm which statistically selects the immobile elements by identifying the maximum number of elements compatible with the same isocon within their 1σ standard deviation uncertainties in concentration. In the considered case studies of the present paper, this approach was used by Goncalves et al. (2012).

Although the use of these geochemical approaches provides information on absolute element mobility during fluid-rock interactions (e.g., Gresens, 1967; Grant, 1986), for a comprehensive ductile shear zone petrological analysis, these data must be accompanied by the determination of stable mineral assemblages in response of element gains and losses. Thermodynamic software using internally consistent databases, e.g., THERMOCALC (Holland and Powell, 1985; Powell and Holland, 1988), Gibbs (Spear and Menard, 1989), PerpleX (Connolly, 1990, 2005) and Theriak-domino

(de Capitani and Petrakakis, 2010) allow the calculation of equilibrium phase diagrams, e.g. pseudosections. Pseudosection calculations (e.g., isothermal pressure vs bulk composition variations, i.e., P-X, isobaric temperature vs bulk composition variations, i.e., T-X, and isothermal and isobaric chemical potential variations diagram, i.e., μ-μ) for ductile shear zones enables to detect changes in bulk rock composition, the set-up of chemical potential gradients and to establish the P-T conditions at which mineral assemblages equilibrate in response to bulk rock composition changes during fluid-assisted mylonitization (e.g., Selverstone et al., 1991; Oliot et al., 2010; Raimondo et al., 2011; Sanchez et al., 2011; Goncalves et al., 2012; Maggi et al., 2014; Tsunogae and van Reenen, 2014; Diener et al., 2016). As an example, the T-X$_{bulk\ rock\ composition}$ pseudosection at a fixed pressure of 7 kbar constructed by Tsunogae and van Reenen (2014) has been here considered (Figure 3). X=0 refers to the
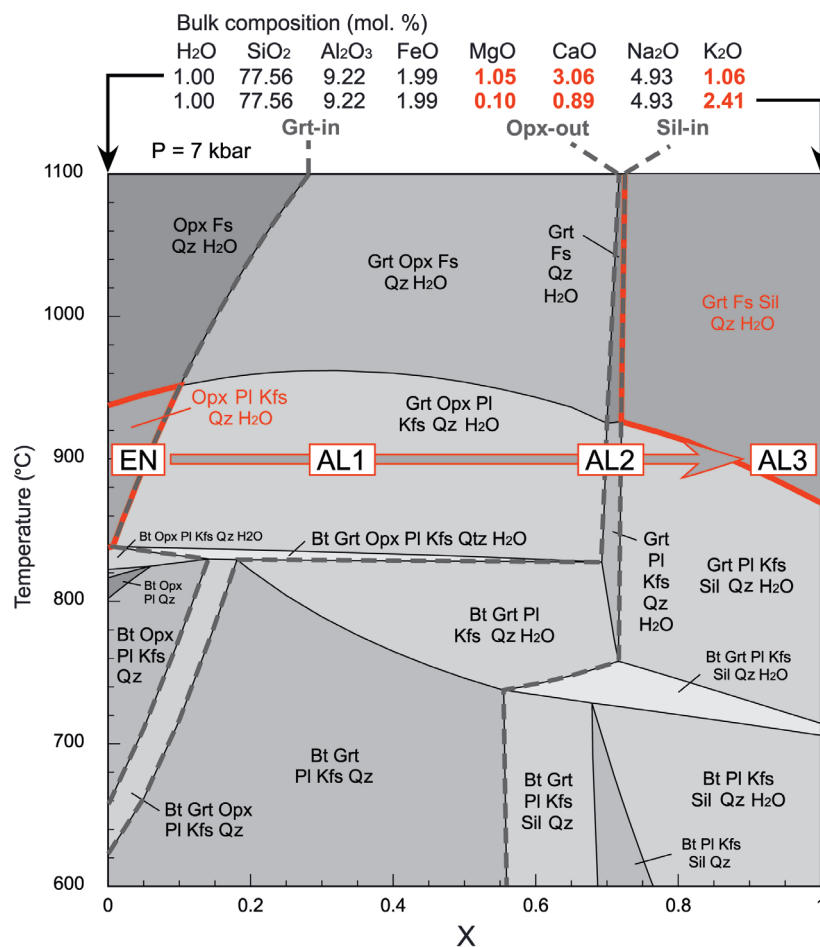

Figure 3. T-X pseudosection showing the stability relations of mineral assemblages in felsic rock samples named EN, AL1, AL2, and AL3 as a function of increasing chemical modification (modified after Tsunogae and van Reenen, 2014). Mineral abbreviations from Whitney and Evans (2010).

bulk rock composition of the unaltered protolith while, X=1 refers to the bulk rock composition of the chemically modified rock. This type of pseudosection allows to investigate the stability fields of different mineral assemblages by varying T and X or, by varying X fixing T and vice versa. In this way, the effective sequence of mineral assemblages passing from the unaltered protolith (X=0) to the chemically modified rock (X=1) has been obtained as well as the P-T conditions (net of some thermobaric uncertainties, as discussed in Fazio et al., 2008) of the fluid-rock interaction process (Figure 3).

The time-integrated fluid flux

A suitable continuum model to simulate the appropriate physical conditions for the metamorphic fluid-rock interaction is based on reactions between the rock and the fluid flowing through it. By considering a one-dimensional continuum model, where a fluid flows through a porous rock column having a unit-cross sectional area and a long axis oriented parallel to the fluid flow direction, two main mechanisms are considered to produce fluid-rock reactions during fluid infiltration (Ferry and Gerdes, 1998). One is a reaction-driven by an infiltrating fluid in chemical disequilibrium with the pervaded rock; the other is a fluid-rock disequilibrium induced by the development of temperature and pressure gradients along the fluid path. Therefore, as the fluid in disequilibrium flows through the rock and promotes devolatilization reactions, the amount of fluid volume/rock area/time differs from point to point along the path as reactions produce or consume fluid species (Dipple and Ferry, 1992; Ferry and Gerdes, 1998).

In order to calculate the quantity of the fluid that pervaded ductile shear zones and promoted fluid-rock reactions inducing chemical modifications in the sheared rocks with respect to their unsheared protoliths, Dipple and Ferry (1992) derived the following equation for chemical variations in the fluid induced by temperature and pressure gradients along the fluid path for a one-dimensional continuum model:

$$q_m = n_i / [(\partial X_i / \partial T)_P (dT/dz) + (\partial X_i / \partial P)_T (dP/dz)] \qquad (3)$$

where q_m is the time-integrated fluid flux (in fluid moles/cm^2), n_i are the total moles of the i species gained or lost by the fluid per rock cm^3, $(\partial X_i / \partial T)_P (dT/dz)$ and $(\partial X_i / \partial P)_T (dP/dz)$ are the variations in concentration of species in the fluid for temperature and pressure gradients along the fluid direction, z.

As n_i can be linked to the solubility of the species in the water, which is a function of temperature and pressure, constrained values of mineral solubility in water, as for the case of SiO$_2$ (Qz), at different temperature and pressure (Walther and Helgeson, 1977; Fournier and Potter, 1982;

Wood and Walther, 1986), can be used to determine time-integrated fluid fluxes (in m^{3}m^{-2}). Therefore, by estimating the amount of quartz enrichment in ductile shear zones, the equation derived by Ferry and Dipple (1991) can be used:

$$qm = \Delta m_{SiO_2} \cdot (\rho_{(rock)} / m_{(rock)}) \cdot (\delta X \rho_{(water)} / \delta Z)^{-1} \qquad (4)$$

where ρ is the density, m is the mass of the shear zone (in g), $\delta X \rho / \delta Z$ is the solubility of quartz in water (as g_{SiO_2} / kg_{H_2O}).

In the case studies considered by the present paper, estimates of the time-integrated fluid fluxes in ductile shear zones have been made by Selverstone et al. (1991), Streit and Cox (1998), Cartwright and Buick (1999) and Rolland and Rossi (2016).

LITERATURE DATASET

We built a synoptic table (Table 1) with the aim to display the major element mobility within ductile shear zones, in relation to the following data: wall rock and ductile shear zone lithotypes and mineral assemblages, dominant tectonic context for shearing, P-T conditions of shearing, and fluid source location. The data derive from those available case studies focusing on major element mobility within ductile shear zones involving felsic protoliths, allowing to calculate chemical variations between the chemically unmodified protoliths and the chemically modified sheared rocks. Therefore, we excluded those other case studies that, while dealing with ductile shear zones in felsic rocks, did not contemplate systematic analysis on bulk rock chemical modifications due to major element mobility during shearing. It follows that, our choice deals with the highest number of possible case studies allowing our attempt to recognize potential common features in terms of major element mobility within ductile shear zones.

Ductile shear zones developed in felsic protoliths
The Tauern Window Shear Zone, Eastern Alps, Northern Italy-Austria

Within the Tauern Window, a deep-crust shear zone developed during Eocene Alpine tectonics overprinting Hercynian metagranodiorites belonging to the Zentralgneiss Unit (Selverstone et al., 1991). Selverstone et al. (1991) recognized the development of four chemically modified zones, where mineralogy changed, from the wall-rock (zone I) to the core of the shear zone (zone IV). The mineral assemblage in the first zone (i.e., in the wall-rock), an unaltered metagranodiorite, was characterized by: (I) Pl + Or + Qz + Bt + Ph + Grt ± Ilm ± Rt ± Aln ± Zrn (hereafter, mineral abbreviations as in Whitney and Evans, 2010), which passed, in the second zone, to a (II) Bt + Ph + Pl + Qz + Grt schist. The third zone consisted of a (III) Bt + Ph ± Pl ± Qz schist, while

the fourth zone, is constituted by a schist containing (IV) Grt + Chl + St ± Bt ± Pl ± Cal. Selverstone et al. (1991) applied the isocon analysis of Grant (1986) to estimate major element changes, in terms of gains and losses from the bulk-rock composition of zone I to the ductile shear zone (zone IV). By this way, Selverstone et al. (1991) observed an overall gain in Fe, Mg and Ti and loss in Si and Ca, with Al being almost immobile, although a relative increase in its amount has been recognized from zone II to IV as function of loss in the other major elements. Selverstone et al. (1991) believe that the increase in Al is responsible for the development of staurolite in zone IV, while the gain in Ca within the ductile shear zone seems not to be linked to any balanced mineral reaction from zone I to zone IV. Therefore, changes in structural domains and mineral assemblages within the ductile shear zone have been associated to the occurrence of mass transfer processes during shearing at 1000 MPa and 550 °C conditions. These processes happened in response to fluid fluxes $\geq 10^8$ m^3m^{-2} from a fluid source located in the shear zone far-field, likely the regionally underthrusted Flysch nappe beneath the Penninic subduction zone.

The Sopron-Fertöàkos area, Eastern Alps, Western Hungary

In the Sopron-Fertöàkos area (western Hungary), the cropping out Sopron Hill metamorphic complex is mainly constituted by orthogneisses and micaschists, with minor leucophyllites and Ky-bearing quarzites (Demény et al., 1997). The orthogneisses developed during Alpine metamorphism, as a product of formerly intruded Variscan granites (Demény et al., 1997). According to Demény et al. (1997), during Alpine orogeny, a shear zone system developed within orthogneisses as a consequence of thrusting on the Penninic units. These Authors reported the development of a series of structural domains from the weakly deformed metagranite to the sheared orthogneiss, and the formation of leucophyllites within ductile shear zones at pressure and temperature conditions of 1300 MPa and 560±30 °C. Demény et al. (1997) argued that leucophyllites developed as consequence of bulk chemical modification of the former metagranite in response to fluid-rock interaction during shearing. Particularly, the Qz + Kfs + Pl + Ms + Bt ± Ap ± Grt ± Rt ± Czo mineral assemblage of metagranites changed to Ph + Mg-Chl + Qtz ± Ky in leucophyllites due to infiltration of an H_2O-rich fluid coming from the ductile shear zone far-field. The application of the isocon method of Grant (1986), allowed Demény et al. (1997) to estimate an overall gain in Mg and K and a loss in Ca, Na, Fe and Si in the ductile shear zone with respect to the metagranitic protolith.

The Moeda-Bonfim Shear Zone, Brazil

The Moeda-Bonfim shear zone crops out in the southern São Francisco craton in southeast Brazil, within the Quadrilatero Ferrifero granite-greenstone terrain which is mainly characterized by Archean granitic-gneissic-migmatitic complexes, Archean metavolcanites and a Proterozoic metasedimentary cover (Hippertt, 1998, and references therein). According to Hippertt (1998), the Moeda-Bonfim ductile shear zone developed during extensional tectonics at 1.0 Ga, within metagranitoid rocks, at greenschist facies shearing conditions of 400 MPa and 400-450 °C. The mylonitic zone is characterized by chemical modifications and changes in mineral assemblages moving from the chemically unmodified metagranite to the chemically modified sheared rocks. On the basis of changes in mineral assemblages and microstructures, Hippert (1998) subdivided the Moeda-Bonfim ductile shear zone in five subzones: (I) Kfs + Qtz + Pl + Bt metagranite; (II) Ms + Kfs + Pl + Qtz ± Chl ± Bt orthogneiss; (III) Ms + Qtz + Chl + Kfs ± Pl orthogneiss; (IV) Ms + Qtz + Chl ± Kfs ± Pl orthogneiss and (V) Ms + Chl + Qtz phyllite. The Author attributed bulk chemical variations and mineral assemblage changes from subzone I to V as consequence of the activation of mass transfer processes from the host-rocks toward the ductile shear zone, in response to the infiltration of an H_2O-rich fluid coming from the shear zone far-field. The application of the isocon analysis of Grant (1986) allowed Hippertt (1998) to determine an overall gain in Si, Fe and K and a loss in Ca and Na in the chemically modified sheared protolith as consequence of fluid-rock interaction.

The King Island Shear Zone System, Tasmania

In King Island, ca. 348±4 Ma, a shear zone system developed at mid-crustal depths on Proterozoic metagranitoids, conditioned by pervasive infiltration of a far-field derived low $\delta^{18}O$-fluid (Streit, 1994; Streit and Cox, 1998). Streit and Cox (1998) investigated fluid-rock interactions and changes in mineral assemblages in two shear zones of the system, at different localities. The growth of new metamorphic Bt and Ph, Ep and Tnt crystals indicated that deformation took place under greenschist facies conditions at 400 to 500 °C and 550 to 750 MPa. Despite the same protolith for the two shear zones, different mineral compositions and bulk rock chemistries developed. In this regard, Streit and Cox (1998) applied the isocon analysis of Grant (1986) to mylonitic samples with respect to the undeformed protolith and deduced different chemical transformations in the two shear zones. Therefore, a gain in Ca and a loss in K, Na and Si have been defined for the northernmost shear zone; while a gain in Na and Si and loss in Ca, Mg and Fe^{3+} have been established for the southernmost shear zone, which was subjected to fluid fluxes of 10^6 m^3m^{-2}.

The Zawidów Granodiorite Shear Zone, Poland

The Zawidów Granodiorite is a Proterozoic biotite-bearing granodiorite cropping out in the eastern part of the Lusatian Granodiorite Complex (Poland) (Bialek, 1999, and references therein). Within the Zawidów Granodiorite, a retrograde shear zone system developed during Variscan orogeny under greenschist to lower-amphibolite facies conditions (Bialek, 1999). According to Bialek (1999), a systematic change in mineral assemblages occurred from the weakly deformed Pl + Qtz + Kfs + Bt ± Tnt ± Ap ± Zrc granodiorite to the sheared protoliths in ductile shear zones, where Qtz + Ms + Chl ± Bt ± Kfs orthogneisses developed. These changes in mineral assemblages were attributed by Bialek (1999) to channelization of H_2O-rich fluids, derived by the occurrence of devolatilization reactions from the host-rocks toward the ductile shear zone, at increasing strain rates. The application of the isocon method of Grant (1986) and mass balance calculation allowed Bialek (1999) to estimate an overall gain in Si, Fe and Na and a loss in Ca and K in the ductile shear zones with respect to the undeformed protoliths.

The Reynolds-Anmatjira Ranges, central Australia

The Reynolds Range is a polymetamorphic terrane mainly composed by greenschist to granulite facies metapelites, metagranitoids (granitic-orthogneisses), quartzites and marbles (Cartwright and Buick, 1999, and references therein). During the Alice Spring Orogeny (450-300 Ma) two sets of thrust-related shear zone systems, having different metamorphic grade, developed within metapelites and metagranitoids, respectively (Cartwright and Buick, 1999). Particularly, ductile shear zones developed within metagranitoids are characterized by mineral assemblages equilibrated under greenschist facies conditions of 400-650 MPa and 420-535 °C (Cartwright and Buick, 1999). According to Cartwright and Buick (1999), systematic mineral assemblage variations can be observed moving from the unsheared granitic-orthogneisses toward the ductilely sheared rocks. In detail, the Kfs + Pl + Qtz + Bt mineral assemblage of the unsheared granitic-orthogneisses passes to (I) Qtz + Kfs + Ms + Bt + Chl + Pl in the moderately sheared rocks, (II) Qtz + Ms + Bt + Chl + Kfs + Pl in the sheared rocks and (III) Qtz + Ms + Chl ± Ksp in the highly sheared one. Cartwright and Buik (1999) attributed this mineral assemblage variation to infiltration of H_2O-rich fluids from a meteoric reservoir, as indicated by low isotopic $\delta^{18}O$ and δ^2H values in sheared rocks, with an estimated time-integrated fluid flux of ca. $4.2 \cdot 10^{-5}$ m^3m^{-2}. These fluid fluxes produced an overall gain in Si and K and a loss of Ca and Na, estimated by the Authors through the application of the isocon analysis of Grant (1986).

The Spruce Lake Nappe Shear Zones, Northern New Brunswick, Canada

The Spruce Lake nappe, in northern New Brunswick, is mainly characterized by a series of dacitic to rhyolitic volcanic rocks that experienced two phases of fluid-rock interaction in response to fluid channeling along a shear zone system, with interacting fluids being alkali-rich (van Staal et al., 2001). Shear zones formed at 600 to 800 MPa and 330 to 370 °C conditions in a compressive tectonic setting, where volcanic rocks, incorporated into the Brunswick complex, were uplifted through the development of an out-of-sequence thrust system (e.g. van Staal et al., 1990, 2001). Van Staal et al. (2001) investigated major element mobility through the isocon analysis of Grant (1986) and highlighted an early stage of interaction between the shearing rocks and a Na-rich fluid in the roof-thrust ductile shear zone, which promoted a weakening effect with widespread albitisation of former Pl and alkali-feldspar, gaining Na, Fe and Mg and loosing K and Si. A later, not pervasive, interaction between deforming rocks and a K-rich fluid promoted the replacement of albite by K-feldspar and allowed the development of Ph-rich phyllonites, with an overall gain in K and Mg and a loss in Na in the basal ductile shear zone. Van Staal et al. (2001) suggested that the responsible fluid sources have been located in the host-rocks (hangingwall and footwall) of the shear zones, delimiting the Spruce Lake nappe.

The Ile d'Yeu Shear Zone System, Armorican Massif, France

The Ile d'Yeu is situated in the southern part of the Armorican Massif belt where orthogneisses of granodiorite, syenogranite and porphyric granite compositions and amphibolite/granulite facies migmatitic paragneiss crop out (Sassier et al., 2006, and references therein). According to Sassier et al. (2006) the two units juxtaposed during stacking of the Armorican Variscan belt with thrusting of the orthogneisses on the paragneisses, when paragneisses experienced peak metamorphic conditions and partial melting at ca. 500 MPa and 600-700 °C (Semelin and Marchand, 1984; Jones and Brown, 1990; Sassier et al., 2006). During thrusting, a shear zone system developed within orthogneisses. Ductile shear zones are characterized by chessboard quartz recrystallization microstructures, and mineral and chemical modification with respect to their protolith (Sassier et al., 2006). Particularly, Sassier et al. (2006) identified the development of sin-kinematic kyanite in response to mineral assemblage changes from slightly peraluminous Qtz + Pl + Kfs + Bt ± Ms ± Grt orthogneisses to Bt + Ms + Qtz + Ky + Ap aluminous schists. Through $\delta^{18}O$ isotopic investigations in chemically unmodified orthogneisses and mylonites, Sassier et al. (2006) argued that the fluid source that enabled chemical modifications within ductile

shear zones was located in the underthrusted migmatitic paragneiss. The application of the isocon method of Grant (1986) allowed the Authors to determine an overall gain in Mg, K and H_2O and a loss of Ca and Na in ductilely sheared orthogneisses.

The Fibbia Metagranite Shear Zone System, Gottard Massif, Swiss Central Alps

A shear zone system developed within Variscan granite intrusives in the Gottard Massif during late Alpine deformation at the Oligocene-Miocene boundary (Challandes et al., 2008, and references therein). Deformation took place under greenschist and amphibolite facies conditions, in the northern and southern boundaries of the Gotthard Massif, respectively (Frey et al., 1974, 1980; Steck, 1976; Le Goff, 1989; Frey, 1999; Labhart, 1999). Oliot et al. (2010) investigated a shear zone developed in the southern Gotthard Massif within the Fibbia metagranite, where weakly deformed metagranite changed to orthogneiss, mylonite and finally to Ab-Zo-bearing ultramylonite. Oliot et al. (2010) related the changes in mineral modes and formation of Ab, Zo and Pl within the ductile shear zone to mass transfer processes. These processes occurred during shear zone formation at almost constant volume conditions, as Oliiot et al. (2010) inferred from the application of the Gresens's (1967) equation. Hence, application of the Gresens's (1967) constant volume equation allowed Oliot et al. (2010) to constrain major element mobility during rock interaction with an H_2O-rich fluid having far-field provenance, resulting into an overall gain in Ca, Fe and Mn. Through the calculation of P-T, T-M_{H2O} and T-$X_{bulk\ composition}$ pseudosections, shearing conditions were constrained at 730±50 MPa and 490±15 °C.

The Reynolds-Anmatjira Ranges, Alice Springs Orogen, Central Australia

A shear zone system, dominated by compressive tectonics, developed during the later stages of Alice Springs Orogeny (450-300 Ma) and dissected the high-grade crystalline basement of the Reynolds-Anmatjira Ranges (Raimondo et al., 2011). Shear zones are characterized by retrogressed, and chemically transformed mineral assemblages, compared to their high-grade protoliths. Raimondo et al. (2011) investigated the fluid-rock interaction and major element mobility during shearing, through the application of the isocon method of Grant (1986, 2005) in traverses crossing two different shear zones of the system. Their traverse 2 showed changes in mineral assemblages from an undeformed granitic gneiss, constituted by (i) Perthite + Pl + Qz + Grt + Bt ± Sil ± Aln, to protomylonitic orthogneiss, consisting of (ii) Perthite + Qz + Bt + Grt, and finally to mylonitic orthogneiss, characterized by (iii) Bt + Qz + Perthite + Grt and (iv) Chl + Bt + Rt ± Qtz. Shearing occurred at 500 ± 150 MPa and 525±26 °C conditions. In both shear zones, changes in mineral assemblages have been associated to fluid-induced bulk rock modification, in response to fluid infiltration from a meteoric reservoir, deduced by $\delta^{18}O$ and δD values. The chemical transformation along traverse 2 resulted into a gain in Fe, Mg, Al, Ti and K as well as a loss in Si, Ca and Na.

The Grimsel Granodiorite Shear Zone System, Aar Massif, Swiss Central Alps

Late Alpine deformation (21-17 Ma) under 450±30 °C and 600±100 MPa conditions was responsible for the development of a ductile shear zone system within the Grimsel granodiorite in the Aar Massif, Central Alps (e.g. Fourcade et al., 1989; Challandes et al., 2008; Rolland et al., 2009). According to Goncalves et al. (2012) a network of phyllosilicate-rich, centimetric to decametric localized shear zones developed surrounding undeformed granodiorite lenses. A sequence of structural and lithological modified products from the undeformed protolith to Chl-Ph bearing ultramylonites, passing from orthogneiss to mylonites was recognized. Goncalves et al. (2012) applied the statistical approach of Baumgartner and Olsen (1995) for mass balance calculations and determined an overall gain in Mg and H_2O, and loss in Ca and minor Na. Through the calculation of isobaric-isothermal μ-μ diagrams at P=650 MPa and T=450 °C, Goncalves et al. (2012) related the shear zone widening and the formation of Chl and Ph in ultramylonites to the chemical instability of the mineral assemblage constituting the undeformed protolith during deformation accompanied by fluid influx.

The East Tenda Shear Zone, Corsica

The East Tenda Shear Zone (ETSZ) is a major Alpine shear zone, formed in response to Africa-Eurasia convergence during Eocene times (Vitale Brovarone et al., 2013; Maggi et al., 2014). The ETSZ juxtaposed the oceanic-derived Schistes Lustrés nappe onto the Variscan crystalline basement, basically constituted by the Casta granodiorite (Daniel et al., 1996; Molli et al., 2006; Martin et al., 2011; Maggi et al., 2012; Maggi et al. 2014). Maggi et al. (2014) investigated the changes in mineralogy and rheology within the shear zone, in response to the interaction between shearing rocks and alkali-rich fluids coming from the overthrusted Schistes Lustrés, which promoted bulk rock modification at 400 MPa and 300 °C. The development of five structural/lithological domains has been associated to five progressive steps of rheological evolution within the former Casta granodiorite. During rheological evolution, the development of Na-Amp bearing/Kfs poor shear zones, Kfs-rich shear zones and Ph-rich phyllonitic shear zones, documents an overall gain in Na, K, Mg and H_2O and loss in Ca, which have been inferred by the application of the isocon method of Grant (1986, 2005).

The Southern Marginal Zone, Limpopo Complex, South Africa

The Southern Marginal Zone (SMZ) is part of the Limpopo Complex (South Africa) and comprises mafic and felsic (enderbite) granulites (e.g. Du Toit et al., 1983). It is internally dissected into several crustal blocks by high-grade shear zones, which are part of the Hout River Shear Zone System developed ca. 2.69-2.62 Ga, and controlled exhumation of the granulitic terrane during Neoarchean collision between the Zimbabwe Craton and the underthrusted Kaapval Craton (e.g., Mason, 1973; Van Reenen et al., 1987; Roering et al., 1992). Within the SMZ, Tsunogae and Van Reenen (2014) investigated the changes in mineralogy within the Petronella Shear Zone-hosted block, which experienced K-rich fluid/rock interaction slightly after peak granulite facies metamorphic conditions. Particularly, the unaltered protolith is made up by an orthopyroxene-bearing quartz-feldspathic gneiss (enderbite), while the chemically transformed rock type is a Qz-Fsp gneiss. A modified sequence of mineral assemblages comprising: (i) Pl + Qz + Opx + Kfs ± Mag ± Ilm ± Rt, (ii) Pl + Qz + Kfs + Grt, and finally (iii) Mesoperthite/Antiperthite + Qz + Kfs + Grt + Sil was established. The occurrence of the chemically modified zones during thrust-related exhumation at 700 MPa and 900 °C, deduced throughout the construction of P-T and T-$X_{bulk\ composition}$ pseudosections, produced a gain of K and a loss of Ca, Mg, Fe, Na and Ti within the shear zone. Tsunogae and Van Reenen (2014) suggested that the fluid source which promoted the chemical transformation of the orthopyroxene-bearing enderbite can be attributed to dehydration of the underthrusted Kapvaal Cratoon.

The Kuckaus Mylonite Zone, Namibia

The Kuckaus Mylonite Zone is a segment of the retrograde Marshall Rocks-Pofadder shear zone system developed ca. 1005-960 Ma, in rocks that experienced granulite facies peak metamorphic conditions ca. 1200-1050 Ma (Diener et al., 2016, and references therein). Diener et al. (2016) investigated P-T conditions of deformation in the Kuckaus Mylonite Zone, which developed in sheared orthogneiss with minor enclaves and lenses of retrogressed mafic granulites. The Hbl + Pl + Qz mafic lenses show a microstructural evolution from the core to the mylonitic rim, with (i) grain size reduction of plagioclase and hornblende, (ii) increase in chlorite and epidote modes, with chlorite foliae forming an interconnected network and, (iii) decreasing X_{an} in plagioclase cores (i.e., X_{an}=0.68, 0.57 and 0.47) from the undeformed lens core toward the mylonitic rim. They related these variations to water gain during deformation from a supposed, far-field meteoric reservoir. Calculations of P-T and T-M_{H_2O} pseudosections allowed Diener et al. (2016) to constrain shearing conditions between 270 to 420 MPa and 450 to 480 °C.

The Mont Blanc Shear Zone System, North-Western Alps, Italy-France

The Mont Blanc Massif pertains to the Variscan External Crystalline Massifs of the NW Alps and is constituted by early-Paleozoic paragneisses, orthogneisses and migmatites, which where intruded by late-Variscan calc-alkaline granitic magmas (e.g., Rolland and Rossi, 2016 and references therein). During Alpine orogeny, a shear zone system developed within the Mont Blanc Massif, characterized by the development of subvertical, transpressive shear zones and cataclastic zones connected by subhorizontal "episyenite" veins (Rolland et al., 2003; Rossi et al., 2005). Ductile shear zones and cataclastic zones are all constituted by greenschist facies mineral assemblages. Moving from the outer to the inner part of the granitic batholith, Rossi et al. (2005) distinguished four main shear zone mineral assemblages: (i) Ep-bearing mineral assemblages in the north-western part of the batholith, (ii) Ms-Bt-Tnt-bearing assemblages in the south-eastern part, (iii) Act-Ms-bearing assemblages in the central-eastern part and (iv) Phl-rich Chl-bearing mineral assemblages in the center of the massif.

On the basis of mineral chemistry variations, i.e. lower X_{Fe} in biotites and chlorites in the inner Massif shear zones with respect to the outer, dating of syn-kinematic phlogopites, phengites and biotites (Rolland et al., 2008), and mass balance calculations, Rolland and Rossi (2016) concluded that shear zones in the Mont Blanc Massif developed during two subsequent deformation stages. The first stage was characterized by ductile shearing at 32-29 Ma and the second by brittle-ductile at 22-14 Ma. Particularly, the first deformation stage occurred at peak metamorphic conditions of 500±100 MPa and 450 °C during underthrusting of the Mont Blanc Massif under the Penninc Front (Rolland and Rossi, 2016). The application of the isocon analysis of Grant (1986) to estimate major element changes from unmodified metagranite to chemically modified Phl-bearing shear zones, allowed Rolland and Rossi (2016) to perform mass balance calculations. They deduce an overall gain of Mg and Fe, and a loss of Si, Ca, Na and K, during the first stage of ductile shearing, in response to the interaction between the metagranite and an upgoing Fe, Mg-rich Si-undersaturated deep seated fluid pervading the shear zone with fluid fluxes of 2-4·10^6 m^3m^{-2}.

INSIGHTS ON MAJOR ELEMENT MOBILITY
Major element mobility in relation to fluid flux

Values in the range of 10^5-10^8 m^3m^{-2} of time-integrated fluid fluxe characterize some of the case studies considered by the present paper; more in detail, values in the order of 10^5-10^6 m^3m^{-2} have been calculated by Streit and Cox (1998), Cartwright and Buick (1999) and Rolland and Rossi (2016) for ductile shear zones

PM

developed under greenschists facies conditions, whereas a value of 10^8 m^{3}m^{-2} has been obtained by Selverstone et al. (1991) for a ductile shear zone developed at higher pressures of the transition between greenschists and amphibolite facies conditions. These values fall within the field of time-integrated fluid fluxes indicated by Dipple and Ferry (1992) able to promote metasomatism within ductile shear zones. Therefore, since in these case studies all the major elements are mobilized (except for Al and Mn; see Table 1), the mobilization of preferred major elements seems not related to fixed values of a time-integrated fluid flux. Thus, if the selection of major elements by the fluid has to be found in other chemical or physical properties of the fluid itself, some direct relation is expected between the amounts of the fluid flux and of the mobilized selected major elements (e.g., Selverstone et al., 1991; Streit and Cox, 1998; Cartwright and Buick, 1999; Rolland and Rossi, 2016). Hence, larger volumes of chemically modified felsic protoliths during ductile shearing occurred under greenschists - amphibolite facies conditions, generally characterized by a higher circulation of fluids, rather than under higher P and/or T conditions, which are typically drier (e.g., Etheridge et al., 1983; McCaig, 1988; Wintsch et al., 1995).

Major element mobility in relation to thermobaric conditions and tectonic context

In order to investigate in as much as the thermobaric conditions exert a control on the mobility of major elements within ductile shear zones, the P-T diagrams of Figures 4 and 5 have been constructed in terms of gains and losses of major elements in felsic systems. In addition to the fifteen case studies shown in Table 1, further two ductile shear zones developed in felsic protoliths, included in Dipple and Ferry (1992), namely Marquer et al. (1985) and Dipple et al. (1990), have been also considered (labeled 16a and 16b, respectively, in Figure 5).

As shown in Figure 4, a common feature for felsic protoliths is the gain in H$_2$O by ductile shear zones developed in different tectonic contexts and P-T conditions. As shown in Figure 5, K, Ca, Na, Mg, Si and Fe exhibit the greatest mobility, while Ti, Al and Mn can be practically considered immobile.

K is almost gained at different metamorphic grades, although some losses occur under greenschist facies conditions (Figure 5). By contrast, Ca is almost lost whatever the metamorphic grade; however, some gains fall in the greenschist facies field (Figure 5). Na is almost lost at different metamorphic grades, although some gains appear under low-grade metamorphic conditions (Figure 5). Mg is always gained from very low- to medium-grade metamorphic conditions, except for two cases of loss under greenschist and granulite facies conditions

(Figure 5). Si shows both gains and losses from low- to medium-T conditions; however, it is preferentially lost at higher pressure conditions (Figure 5). The gain of Fe is typical of the greenschist facies, although two cases of loss under eclogite and granulite facies can be observed (Figure 5).

No remarkable outcomes derive on the mobility of major elements by the tectonic context for shearing, except for the Mg which results almost gained under dominant compressive tectonics (Figure 5).

Major element mobility related to fluid sources

According to Table 1, fluids that infiltrated ductile shear zones mostly have a deep-seated or meteoric provenance, with the reservoirs located in the shear zone "far-field" (Selverstone et al., 1991; Demény et al., 1997; Hippertt, 1998; Streit and Cox, 1998; Cartwright and Buick, 1999; Oliot et al., 2010; Raimondo et al., 2011; Tsunogae and van Reenen, 2014; Rossi and Rolland, 2014; Diener et al., 2016; Rolland and Rossi, 2016). In few cases, the fluid provenance was located in the ductile shear zone "near-field", namely in the host-rocks (Bialek, 1999; van Staal et al., 2001; Sassier et al., 2006; Maggi et al., 2014).

In order to assess the potential relationships between major element mobility within ductile shear zones and fluid sources, we have built a histogram (Figure 6) based on the data shown in Table 1 (see Selverstone et al., 1991; Demény et al., 1997; Hippertt, 1998; Strei and Cox, 1998; Bialek, 1999; Cartwright and Buik, 1999; Sassier et al., 2006; Oliot et al., 2010; Raimondo et al., 2011; Goncalves et al., 2012; Maggi et al., 2014; Tsunogae and van Reenen, 2014; Rolland and Rossi, 2016) and reported in the review paper of Dipple and Ferry (1992; see Marquer et al., 1985; Dipple et al., 1990). Mean weight percentages (wt%) of gained and lost elements have been calculated with respect to the results on the mobilized major elements in the single literature case studies from Table 1, according to the following equation:

$$\Delta wt(\%)_i = [\sum_{k=1}^{n}(m_i^a - m_i^0)_k]/n \qquad (5)$$

Where $\Delta wt(\%)_i$ is the mass variation in percentages of the i species, k is the case study number according to Table 1 that varies from 1 to n, m_i^a is the mass, expressed in wt% of the i species in the chemically modified rock a, and m_i^0 is the mass, expressed in wt% of the i species in the chemically unmodified protolith 0. A value of zero to the difference $m_i^a - m_i^0$ was attributed when no gains or losses were detected through mass balance calculations for the single element between the chemically modified rock and the chemically unmodified protolith, while, positive or negative values were obtained when gain or loss occurred, respectively. Mean weight percentages of gained and lost

Table 1. Ductile shear zones features from literature case studies.

	Wall rock and ductile shear zone lithotypes and mineral assemblages			Dominant tectonics for shearing	P[MPa]-T[°C] conditions of shearing	Major element mobility In ductile shear zones		Fluid source location for major element mobility in ductile shear zones
	Hangingwall	Shear zone	Footwall			Gain	Loss	
1	main lithotype: meta-granodiorite mineral assemblage: Pl + Or + Qz + Bt + Ph + Grt ± Ilm ± Rt ± Aln ± Zrn other lithotype: amphibolite (mafic lenses) mineral assemblage: Hbl + Bt + Czo + Pl	main lithotype: garnet-bearing schist mineral assemblage: Grt + Chl + St ± Bt ± Pl ± Cal	main lithotype: meta-granodiorite mineral assemblage: Pl + Or + Qz + Bt + Ph + Grt ± Ilm ± Rt ± Aln ± Zrn other lithotype: amphibolite (mafic lenses) mineral assemblage: Hbl + Bt + Czo + Pl	compressive	P ≈ 1000 T ≈ 550	Fe, Mg, Ti	Si, Ca	far-field (regionally underthrusted flysch belt)
2	lithotype: metagranite/orthogneiss mineral assemblage: Qz + Kfs + Pl + Ms + Bt + Ap ± Grt ± Rt ± Czo	lithotype: leucophyllites mineral assemblage: Ph + Mg-Chl + Qz ± Ky	lithotype: metagranite/orthogneiss mineral assemblage: Qz + Kfs + Pl + Ms + Bt ± Ap ± Grt ± Rt ± Czo	compressive	P = 1300 T = 560 ± 30	Mg, K, H_2O	Ca, Na, Fe, Si	far-field (regionally underthrusted Penninic complex)
3	lithotype: granite mineral assemblage: Kfs + Pl + Qz + Bt	lithotype: orthogneiss mineral assemblage: Qz + Ms + Chl ± Kfs	lithotype: granite mineral assemblage: Kfs + Pl + Qz + Bt	extensional	P = 400 400 < T < 450	Si, Fe, K	Ca, Na	far-field (generic)
4	lithotype: granodiorite mineral assemblage: Qz + Pl + Kfs + Ms + Bt + Chl	lithotype: orthogneiss mineral assemblage: Kfs + Pl + Bt + Ms + Qz ± Chl ± Tnt ± Ep	lithotype: granodiorite mineral assemblage: Qz + Pl + Kfs + Ms + Bt + Chl		550 < P < 700 400 < T < 500	Ca, H_2O (in Cape Wickham mylonite - a) Na, Si, H_2O (in Disappointment Bay Shear Zone - b)	Na, K, Si (by Cape Wickham mylonite - a) Ca, Fe, Mg (by Disappointment Bay Shear Zone - b)	far-field (deep-seated metamofphic devolatisation?)
5	lithotype: granodiorite mineral assemblage: Pl + Qz + Kfs + Bt + Tnt ± Ap ± Zrn	lithotype: orthogneiss mineral assemblage: Qz + Ms + Chl ± Bt ± Kfs	lithotype: granodiorite mineral assemblage: Pl + Qz + Kfs + Bt + Tnt ± Ap ± Zrn	extensional	P ≈ 500 T ≈ 450	Si, Fe, Na	Ca, K	near-field (host-rock)
6	lithotype: metagranite mineral assemblage: Kfs + Pl + Qz + Bt	lithotype: orthogneiss mineral assemblage: Qz + Ms + Chl ± Kfs	lithotype: metagranite mineral assemblage: Kfs + Pl + Qz + Bt	compressive	400 < P < 650 420 < T < 535	Si, K, H_2O	Ca, Na	far-field (meteoric reservoir)

Table 1. Continued...

	Wall rock and ductile shear zone lithotypes and mineral assemblages			Dominant tectonics for shearing	P[MPa]-T[°C] conditions of shearing	Major element mobility In ductile shear zones		Fluid source location for major element mobility in ductile shear zones
	Hangingwall	Shear zone	Footwall			Gain	Loss	
7	lithotype: metabasite (ophiolite)	lithotype: metavolcanite mineral assemblage: Kfs + Ab + Qz + Ph + Stp + Cal or Na-Amph ± Na-Cpx ± Tnt ± Pmp ± Ep	lithotype: metavolcanites	compressive	$600 < P < 800$ $330 < T < 370$	Na, Fe, Mg (roof - a) K, Mg (base - b)	K, Si (roof - a) Na (base - b)	near-field (hangingwall and footwall)
8	lithotype: orthogneiss mineral assemblage: Qz + Pl + Kfs + Bt ± Ms ± Grt	lithotype: orthogneiss mineral assemblage: Bt + Ms + Qz + Ky + Ap	lithotype: migmatitic paragneiss mineral assemblage: Bt + Pl + Qz ± Crd ± Grt ± Ilm ± Sil ± Ap ± Zrn	compressive	$P = 500$ $600 < T < 700$	Mg, K, H_2O	Ca, Na	near-field (footwall)
9		main lithotypes: orthogneiss and ultramylonitic orthogneiss mineral assemblage: Pl + Qz + Kfs + Bt + Ph ± Zo ± Grt other lithotype: metagranite (unmodified protolith) mineral assemblage: Qz + Kfs + Pl + Bt ± Zo ± Ph ± Ap ± Aln		compressive	$P = 730 \pm 50$ $T = 490 \pm 15$	$H2O$, Ca, Fe, Mn		far-field (generic)
10	lithotype: orthogneiss mineral assemblage: Perthite + Pl + Qz + Grt + Bt ± Sil ± Aln	lithotype (traverse 2): schist mineral assemblage: Chl + Bt + Rt ± Qz lithotype 1: orthogneiss mineral assemblage: Wm + Ab + Ep + Qz + Bt lithotype 2: ultramylonitic orthogneiss	lithotype: orthogneiss mineral assemblage: Perthite + Pl + Qz + Grt + Bt Sil ± Aln	compressive	$P = 500 \pm 150$ $T = 525 \pm 26$	Fe, Mg, Al, Ti, K, H_2O	Si; Ca, Na	far-field (meteoric reservoir)
11		mineral assemblage: Ab + Ph + Qz + Chl + Bt other lithotype: granodiorite (unmodified protolith) mineral assemblage: Pl + Qz + Kfs + Bt		compressive	$P = 650$ $T = 450$	Mg, H_2O	Ca, Na	far-field (deep-seated fluids; Rossi and Rolland, 2014)

Table 1. Continued...

	Wall rock and ductile shear zone lithotypes and mineral assemblages			Dominant tectonics for shearing	P[MPa]-T[°C] conditions of shearing	Major element mobility In ductile shear zones		Fluid source location for major element mobility in ductile shear zones
	Hangingwall	Shear zone	Footwall			Gain	Loss	
12	lithotypes: Schistes Lustrès	lithotype 1: phyllonite mineral assemblage: Ph + Qz + Pl + Kfs + Na-Amp lithotype 2: orthogneiss mineral assemblage: Qz + Pl + Kfs + Ph	lithotype: granodiorite mineral assemblage: Pl + Qz + Kfs + Hbl + Bt ± Tnt ± Ap ± Aln ± Zrn	compressive	P = 400 T = 300	K, Na, Mg, H$_2$O	Ca	near-field (hangingwall, Schistes Lustrès)
13	lithotype: orthogneiss mineral assemblage: Pl + Qz + Opx + Kfs + Bt ± Mag ± Ilm ± Rt	lithotype: orthogneiss mineral assemblage: Meso- and Anti-Perthite + Qz + Kfs + Grt + Sil	lithotype: orthogneiss mineral assemblage: Pl + Qz + Opx + Kfs + Bt ± Mag ± Ilm ± Rt	compressive	P = 700 T = 900	K, H$_2$O	Ca, Mg, Fe, Ti, Na	far-field (regionally underthrusted greenschist facies orthogneiss; mineral assemblage: Pl + Qz + Bt + Mc ± Ep/Czo ± Cb ± Ms ± Aln ± Tnt ± Ilm ± Mag)
14		main lithotype: orthogneiss mineral assemblage: Hbl + Pl + Qz + Chl ± Ep other lithotype: mafic metapelite (lenses) mineral assemblage (mylonitic rim of the lenses): Pl + Hbl + Chl + Qz ± Ep ± Tnt		extensional	270 < P < 420 450 < T < 480	H$_2$O		far-field (meteoric reservoir)
15	lithotype: metagranite mineral assemblage: Qz + Kfs + Pl + Bt ± Ep ± Chl ± Ms	lithotype (Chl-Phl shear zones): orthogneiss mineral assemblage: Phl + Chl + Qz + Kfs ± Pl	lithotype: metagranite mineral assemblage: Qz + Kfs + Pl + Bt ± Ep ± Chl ± Ms	compressive	P = 500 ± 100 T = 450	Fe, Mg, H$_2$O	Si, Ca, Na, K	far-field (deep-seated fluids)

Notes: - Case studies: 1 Selverstone et al. (1991; Tauren Window Shear Zone, Eastern Alps, Northern Italy - Austria), 2 Demény et al. (1997; Sopron-Fertőákos area, Eastern Alps, Western Hungary), 3 Hippertt (1998; The Boema-Bonfim Shear Zone, Quadrilatero Ferrifero, Brazil), 4 Streit and Cox (1998; King Island Shear Zone System, Tasmania), 5 Bialek (1999; The Zawidów Granodiorite Shear Zone, Poland), 6 Cartwright and Buick (1999; Reynolds–Anmatjira Ranges, Central Australia), 7 van Staal et al. (2001; Spruce Lake Nappe Shear Zone, Northern Brunswick, Canada), 8 Sassier et al. (2006; Ile d'Yeu Shear Zone System, Armorican Hercynian Belt, France), 9 Oliot et al. (2010; Fibbia Metagranite Shear Zones System, Gottard Massif, Swiss Central Alps), 10 Raimondo et al. (2011; Reynolds-Anmatjira Ranges, Alice Spings Orogen, Central Australia), 11 Goncalves et al. (2012; Grimsel Granodiorite Shear Zone System, Aar Massif, Swiss Central Alps), 12 Maggi et al. (2014; East Tenda Shear Zone, Corsica), 13 Tsunogae and van Reenen (2014; Southern Marginal Zone, Limpopo Complex, South Africa), 14 Diener et al. (2016; Kuckaus Mylonite Zone, Namibia), 15 Rolland and Rossi (2016; Mont Blanc Shear Zone, North-Western Alps, Italy-France).

- Fe^{2+} and Fe^{3+} have been treated as Fe$_{tot}$ = Fe.

- Fluid source location for major element mobility in ductile shear zones: far-field and host-rock refer to the the ductile shear zone.

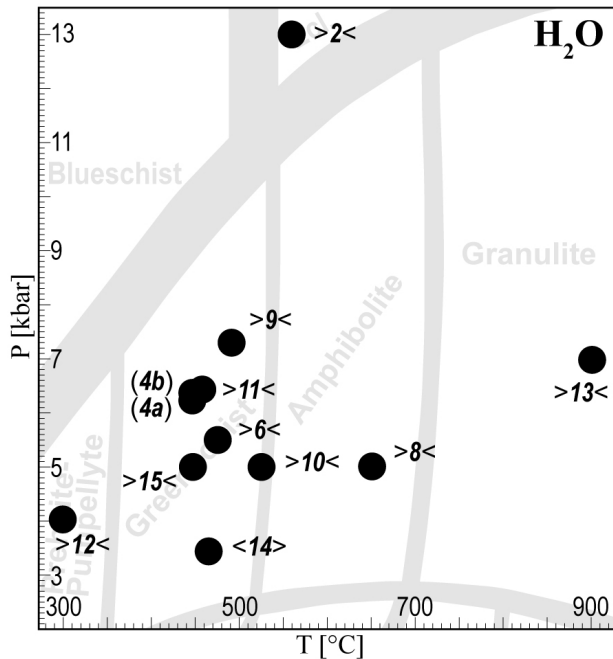- Mineral abbreviations after Whitney and Evans (2010).

PM

Figure 4. P-T diagrams showing H_2O gain (black filled circles) and losses (empty circles) within ductile shear zones developed in felsic protoliths; each number, refers to the literature case studies as in Table 1; convergent angle brackets at sides of numbers of cases studies indicate dominant compressive tectonics; divergent angle brackets at sides of numbers of case studies indicate dominant extensional tectonics; numbers of case studies between parenthesis indicate undefined tectonic context; metamorphic facies fields after Winter (2014).

elements have been calculated for sheared rocks in relation to the fluid source type, i.e., host-rocks or far-field sources relative to the ductile shear zones, whatever the tectonic context for shearing. In these calculations, the wt% of H_2O has not been considered since it likely represents the fluid mean.

Figure 6 shows clearly that Mg and K are almost gained independently of whether the fluid source was located in the host-rocks or in the far-field of the ductile shear zone. A gain in Fe within ductile shear zones occurs when the fluids derived from far-field sources, while in the case of host-rocks sources this element seems to be immobile. An opposite feature regards the Si mobility: it is almost lost when the fluid source was located in the shear zone far-field and gained when it was located in the shear zone host-rocks. Looking to the behavior of Ca and Na, it appears from the histogram in Figure 6 that they are always lost whatever the fluid source is. As regards Al, it shows gains of ca. 0.5 (wt%) in the case of fluids having a far field origin with these gains that can be attributed to mass balance, accounting for Si depletion under the same circumstances (e.g., Selverstone et al., 1991). Ti and

Mn show gains <0.5 (wt%) and therefore can be actually assumed immobile whatever the fluid source.
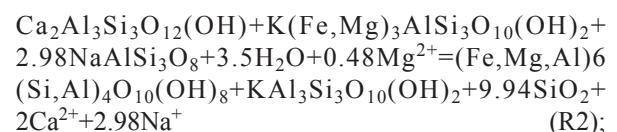
Consequently, some major outcomes from the analysis of major element mobility with respect to fluid sources can be assessed: i) fluids coming from far-field sources with respect to the ductile shear zone mobilize Si, Mg, Fe, Ca, Na and K, with gains in Mg, Fe and K and frequently remarkable losses in Si, Ca and Na; ii) fluids derived from the shear zone host-rocks mobilize Si, Mg, Ca, Na and K, with Si, Mg and K gained and Ca and Na lost.

Fluid-rock interaction and final considerations on the major element mobility

The far-field source for fluids pervading ductile shear zones, has been suggested in several case studies when an incompatibility between the chemistry detected in the sheared rocks and that of the surrounding wall rocks occurred. As a consequence, the relative abundance in K and Na, as well as Ca, Fe, Mg, Si and rarely Ti, Al and Mn within ductile shear zones, has been related to aqueous fluids of undefined provenance or coming from meteoric reservoirs or from deep seated crustal sources (Selverstone et al., 1991; Demény et al., 1997; Hippertt, 1998; Streit and Cox, 1998; Cartwright and Buick, 1999; Oliot et al., 2010; Raimondo et al., 2011; Tsunogae and van Reenen, 2014; Rossi and Rolland, 2014; Diener et al., 2016; Rolland and Rossi, 2016) (Table 1). In all these cases, gain and loss in major elements, in response to fluid-rock interaction during shearing, favored the development of minerals not compatible with the chemistry of the wall rocks. For instance: (i) the development of muscovite-rich and feldspar-poor mineral assemblages in ductile shear zones has been attributed by Hippertt (1998) to gain in K and loss in Ca and Na by the feldspar breakdown reaction (R1) induced by the infiltration of H_2O-rich fluids during shearing:

$(Na,Ca)Al_{1-2}Si_{2-3}O_8+1.5KAlSi_3O_8+0.5H_2O+4H^+$
$=2KAl_3Si_3O_{10}(OH)_2+0.5Ca(Al,Fe^{3+})3Si_3O_{12}(OH)+$
$11SiO_2+4Na^+$ (R1)
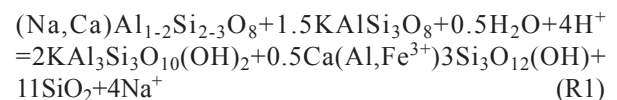
(ii) Chl + Ms mineral assemblages (e.g., Goncalves et al., 2012) and Phl-bearing mineral assemblages (e.g., Rolland and Rossi, 2016;) developed in orthogneisses sheared under greenschist facies conditions in response to gain in Mg and leaching of Ca and Na by a Mg-bearing fluid, through the following reactions:

$Ca_2Al_3Si_3O_{12}(OH)+K(Fe,Mg)_3AlSi_3O_{10}(OH)_2+$
$2.98NaAlSi_3O_8+3.5H_2O+0.48Mg^{2+}=(Fe,Mg,Al)6$
$(Si,Al)_4O_{10}(OH)_8+KAl_3Si_3O_{10}(OH)_2+9.94SiO_2+$
$2Ca^{2+}+2.98Na^+$ (R2);
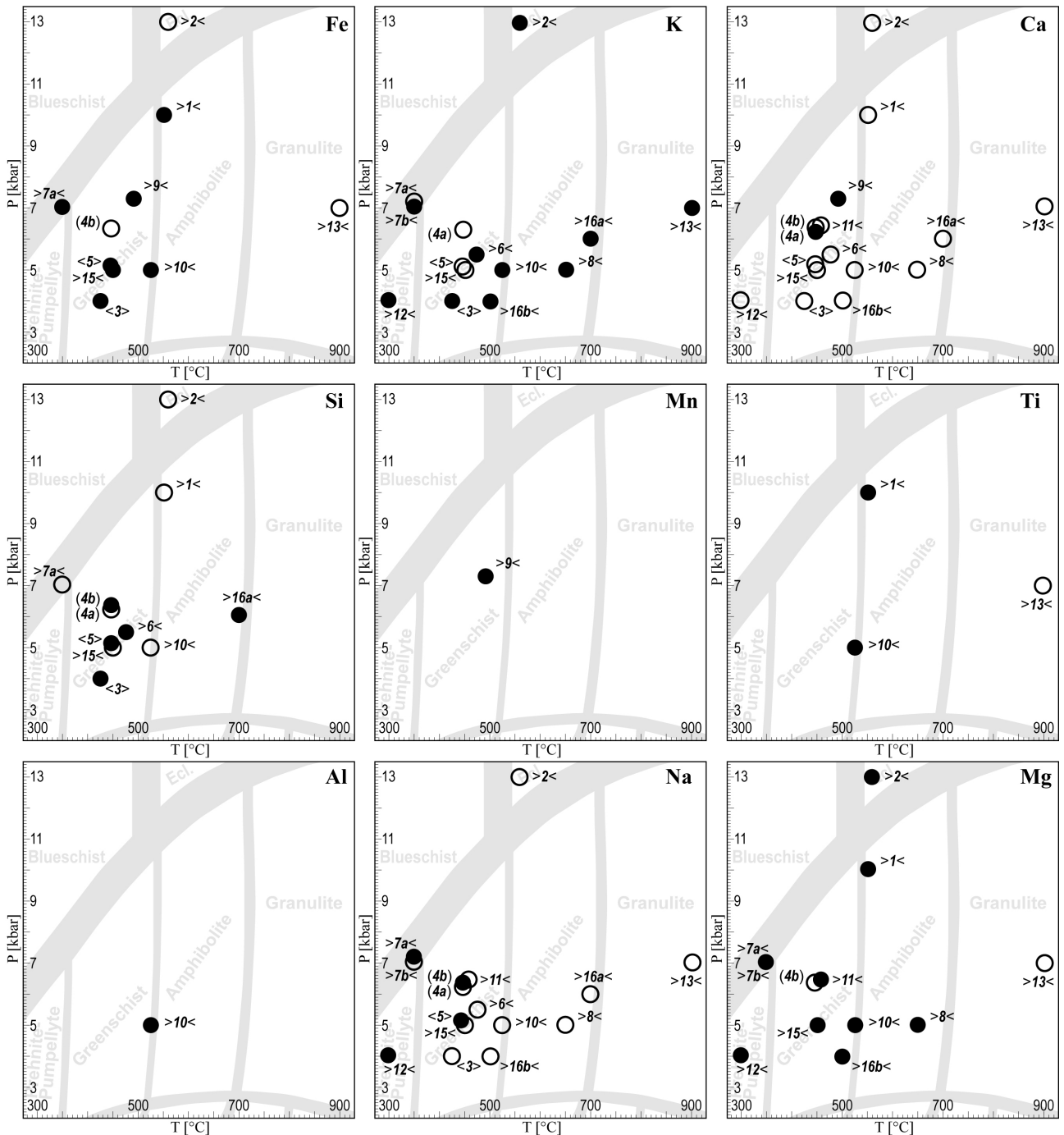
Figure 5. P-T diagrams showing major elements Fe, K, Ca, Si, Mn, Ti, Al, Na and Mg gain (black filled circles) and losses (empty circles) within ductile shear zones developed in felsic protoliths; each number refers to the literature case studies as in Table 1; convergent angle brackets at sides of numbers of case studies indicate dominant compressive tectonics; divergent angle brackets at sides of numbers of case studies indicate dominant extensional tectonics; numbers of case studies between parenthesis indicate undefined tectonic context; 16a and 16b refer to additional case studies in Dipple and Ferry (1992), namely Marquer et al. (1985) and Dipple et al. (1990), respectively; metamorphic facies fields after Winter (2014).
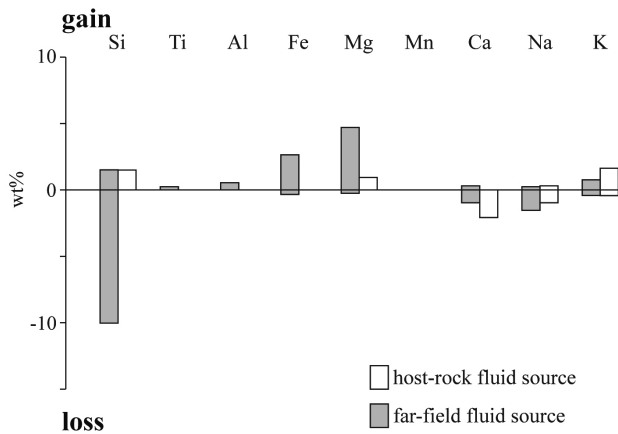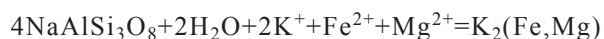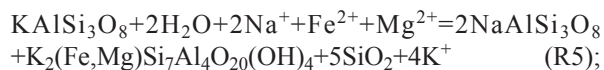
Figure 6. Histogram showing mean weight percentages (wt%) of major element absolute variation from unaltered protolith to chemically modified sheared felsic rocks on the basis of literature case studies in Table 1 (except van Staal at al., 2001) and additional case studies in Dipple and Ferry (1992), namely Marquer et al. (1985) and Dipple et al. (1990).

$$2(Na,Ca)Al_{1-2}Si_{2-3}O_8+K(Fe,Mg)_3AlSi_3O_{10}(OH)_2+SiO_2+KAlSi_3O_8+Fe^{2+}+Mg^{2+}+H_2O=K(Fe,Mg)_3AlSi_3O_{10}(OH)_2+Na^++Ca^{2+}+K^++H_2SiO_4 \qquad (R3)$$
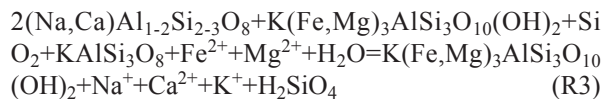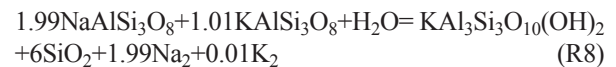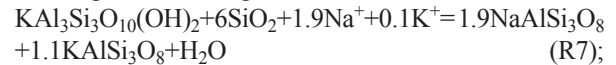
(iii) An-rich plagioclase developed at the expense of a former albite in orthogneiss sheared under upper greenschist facies conditions, in response to gain in Ca (Oliot et al., 2010) through the following reaction:

$$NaAlSi_3O_8+Ca^{2+}+Al_2O_3+2SiO_2=2(Na,Ca)Al_{1-2}Si_{2-3}O_8 \qquad (R4)$$
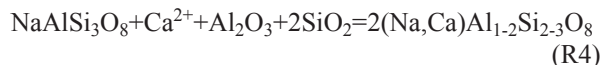
Where some mineralogical compatibility has been observed between mylonites from ductile shear zones and their host-rock, the possible location of the fluid source, that promoted chemical modifications in the investigated ductile shear zones, was located in the nearby host-rocks. For instance: (i) the development of muscovite at the expense of feldspars through the occurrence of reaction R1 was observed by Bialek (1999) in a ductile shear zone set on a granodioritic protolith; (ii) Van Staal et al. (2001) associated the growth of phengite within the sheared felsic protolith to Fe-Mg-rich fluids destabilizing K- and Na-bearing mineral phases in the hangingwall, according to the following rock-fluid reactions:

$$KAlSi_3O_8+2H_2O+2Na^++Fe^{2+}+Mg^{2+}=2NaAlSi_3O_8+K_2(Fe,Mg)Si_7Al_4O_{20}(OH)_4+5SiO_2+4K^+ \qquad (R5);$$

$$4NaAlSi_3O_8+2H_2O+2K^++Fe^{2+}+Mg^{2+}=K_2(Fe,Mg)$$

$$Si_7Al_4O_{20}(OH)_4+5SiO_2+4Na^+ \qquad (R6)$$

(iii) Maggi et al. (2014) associated the formation and dissolution of phengite in the East Tenda Shear Zone, as consequence of K and Na transport by aqueous fluids liberated by the Schistes Lustrès hangingwall (Table 1), promoting the following reaction:

$$KAl_3Si_3O_{10}(OH)_2+6SiO_2+1.9Na^++0.1K^+=1.9NaAlSi_3O_8+1.1KAlSi_3O_8+H_2O \qquad (R7);$$

$$1.99NaAlSi_3O_8+1.01KAlSi_3O_8+H_2O=KAl_3Si_3O_{10}(OH)_2+6SiO_2+1.99Na_2+0.01K_2 \qquad (R8)$$

As stated by reactions R1-R8, the occurrence of specific mineral assemblages in ductile shear zones, whatever the fluid source, is strictly linked to the mobility of some major elements, such as H_2O, Si, K, Fe, Mg, Na and Ca.

More in detail, Si mobility within ductile shear zones is related to the high solubility of quartz into the fluid phase, remarkably when the fluid is pure H_2O (Kennedy, 1950; Walther and Helgeson, 1977; Eugster and Gunter, 1981; Manning, 1994; Harlov and Austrheim, 2013) and even when it contains dissolved salt species as NaCl and $CaCl_2$ (Shmulovich et al., 2006). Thus, the hydrolysis of Qz in H_2O-rich fluids favors the transport of Si in solution through the development of neutral complexes (i.e., H_4SiO_4) (e.g., Walther and Orville, 1983; Harlov and Austrheim, 2013; Manning, 2018). Accordingly, the case studies of Hippertt (1998), van Staal et al. (2001), Raimondo et al. (2011) and Rolland and Rossi (2016) for felsic sheared rocks, reported gains and losses in Si within the ductile shear zones according to reactions R1, R5, R6 and R3, respectively.

As for the case of Si, K, has a high mobility in ductile shear zones as shown in Figure 5. Indeed, it is easily dissolved by H_2O-rich fluids, being almost present in the fluid as K^+ ion species rather than KOH pairs (Manning, 2018). More in detail, its concentrations are slightly sensitive with increasing temperature rather than increasing pressure (Manning, 2018). Therefore, as ductile shear zones are the locus where advection is more important than diffusion, K could be easily transported within them, with its precipitation as mineral phase (e.g., biotite, white mica, amphibole) being related to the P-T conditions at which shearing occurred.

Regarding the mobility of Mg, Fe, Ca and Na, i.e. the relative abundance of Mg-, Fe-, Ca- and Na-bearing minerals in ductile shear zones, this seems to be strictly related to the presence of Cl^- in the fluid. More in detail, Schulien (1980) and Eugster and Gunter (1981) showed that Mg solubility is lower than that of Fe in chloride fluids at thermodynamic equilibrium with Fe-Mg silicates and that Mg is preferentially partitioned into the mineral

phase. Consequently, its gain within ductile shear zones should be more relevant relative to Fe (e.g., Demény et al., 1997; Rolland and Rossi, 2016). This hypothesis is supported by the mean weight percentages of gained Mg and Fe shown in Figure 6. Therefore, gains in H_2O, Fe, Mg and K (Figures 4 and 5) generally cause the formation of phyllosilicates such as white mica, chlorite and biotite within ductile shear zones from greenschist to amphibolite (e.g., Selverstone et al., 1991; Sassier et al., 2006; Rolland and Rossi, 2016) and eclogite facies conditions (e.g., Demény et al., 1997), with their chemistry (e.g., X_{Fe} in biotites and chlorites) being linked to the concentration of Cl^- in the fluid.

Regarding Ca and Na, their concentration in the fluid phase is strictly dependent by the presence of dissolved Cl^- in the fluid. Particularly, the dissolution of albite is enhanced by low concentrations of NaCl in the fluid, while the dissolution of Ca-bearing phases increases markedly at high NaCl concentrations in the fluid (e.g., Manning, 2018, and references therein). Thus, the leaching of plagioclase and Ca-rich garnets in ductile shear zones (see Table 1) may be strongly dependent by the presence of dissolved anions in the fluid.

Therefore, the presence of an H_2O-rich fluid, with a particular chemistry (e.g., different concentrations of dissolved anions and salts), flowing within ductile shear zones (Figure 1), would favor more or less mechanical weakening through the development of particular mineral assemblages (e.g., Etheridge et al., 1983; McCaig, 1988; Selverstone et al., 1991; Wintsch et al., 1995; Ord and Oliver, 1997; Pili et al., 1999; Sassier et al., 2006; Maggi et al., 2014; Diener et al., 2016) whatever the tectonic context and the P-T conditions.

CONCLUDING REMARKS

On the basis of a number of literature case studies, the following qualitative considerations can be forwarded regarding the mobility of major elements in ductile shear zones developed within felsic protoliths:

(i) the mobilization of major elements seems not related to fixed values of time-integrated fluid flux, although large amounts of fluids infiltrating ductile shear zones, produced relevant volumes of chemically modified protoliths;

(ii) no general relations exist between the mobility of major elements and the tectonic context for shearing, except for the Mg, which results almost gained under dominant compressive tectonics;

(iii) a common feature for felsic protoliths is the gain in H_2O by ductile shear zones developed in different tectonic contexts and P-T metamorphic conditions. In addition, K, Ca, Na, Mg, Si and Fe exhibit the greatest mobility, while Ti, Al and Mn can be practically considered immobile whatever P-T metamorphic conditions;

(iv) fluids coming from far-field sources, with respect to the ductile shear zone induced gains in Mg, Fe and K, and frequently remarkable losses in Si, Ca and Na, while fluids derived from the shear zone host-rocks promoted gains of Si, Mg and K, and losses of Ca and Na;

(v) the chemical selection of major elements seems greatly related to the fluid chemistry, and the amounts of fluids seems to play its role in driving at completion the metamorphic fluid-rock reactions within ductile shear zones.

In order to verify the mass transfer within ductile shear zones by fluids of near- or far-field provenance, a mass balance between the materials lost in the wall rocks and gained in the ductile shear zone should be always provided. The feedback of this mass-balance will be directly reflected in pseudosections constructed for ductile shear zones against those constructed for the non-affected wall-rocks; this approach allows to constrain the assessment of chemical potential gradients driven by the fluid-rock interaction, providing strong insights for major element mobility.

REFERENCES

Baumgartner L. and Olsen S., 1995. A least-squares approach to mass transport calculations using the isocon method. Economic Geology 90, 1261-1270.

Bialek D., 1999. Chemical changes associated with deformation of granites under greenschist facies conditions: the example of the Zawidów Granodiorite (SE Lusatian Granodiorite Complex, Poland). Tectonophysics 303, 251-261.

Cartwright I. and Buick I.S., 1999. The flow of surface-derived fluids through Alice Springs age middle-crustal ductile shear zones, Reynolds Range, central Australia. Journal of Metamorphic Geology 17, 397-414.

Challandes N., Marquer D., Villa I.M., 2008. P-T-t modelling, fluid circulation, and [39]Ar-[40]Ar and Rb-Sr mica ages in the Aar Massif shear zones (Swiss Alps). Swiss Journal of Geosciences 101, 269-288.

Connolly J.A.D., 1990. Multivariable phase diagrams: an algorithm based on generalized thermodynamics. American Journal of Science 290, 666-718.

Connolly J.A.D., 2005. Computation of phase equilibria by linear programming: A tool for geodynamic modeling and its application to subduction zone decarbonation. Earth and Planetary Science Letters 236, 524-541.

PM

Daniel J.M., Jolivet L., Goffe B., Poinssot C., 1996. Crustal-scale strain partitioning: Footwall deformation below the Alpine Oligo-Miocene detachment of Corsica. Journal of Structural Geology 18, 41-59.

De Capitani C. and Petrakakis K., 2010. The computation of equilibrium assemblage diagrams with Theriak/Domino software. American Mineralogist 95, 1006-1016.

Demény A., Sharp Z.D., Pfeifer H.R., 1997. Mg-metasomatism and formation conditions of Mg-chlorite-muscovite-quartzphyllites (leucophyllites) of the Eastern Alps (W. Hungary) and their relations to Alpine whiteschists. Contributions to Mineralogy and Petrology 128, 247-260.

Diener J.F.A., Fagereng Å., Thomas S.A.J., 2016. Mid-crustal shear zone development under retrograde conditions: Pressure-temperature-fluid constraints from the Kuckaus Mylonite Zone, Namibia. Solid Earth 7, 1331-1347.

Dipple G.M. and Ferry J.M., 1992. Metasomatism and fluid flow in ductile fault zones. Contributions to Mineralogy and Petrology 112, 149-164.

Dipple G.M., Wintsch R.P., Andrews M.S., 1990. Identification of the scales of differential element mobility in a ductile fault zone. Journal of Metamorphic Geology 8, 645-661.

Du Toit M.C., van Reenen D.D., Roering C., 1983. Some aspects of the geology, structure and metamorphism of the Southern Marginal Zone of the Limpopo metamorphic complex. Special Publication of the Geological Society of South Africa 8, 121-142.

Etheridge M.A., Wall V.J., Vernon R.H., 1983. The role of the fluid phase during regional metamorphism and deformation. Journal of Metamorphic Geology 1, 205-226.

Eugster H.P. and Gunter W.D., 1981. The compositions of supercritical metamorphic solutions. Bulletin de Mineralogie 104, 817-826.

Fazio E., Cirrincione R., Pezzino A., 2008. Estimating P-T conditions of Alpine-type metamorphism using multistage garnet in the tectonic windows of the Cardeto area (southern Aspromonte Massif, Calabria). Mineralogy and Petrology, 93, 111-142.

Ferry J.M. and Dipple G.M., 1991. Fluid flow, mineral reactions, and metasomatism. Geology 19, 211-214.

Ferry J.M. and Gerdes M.L., 1998. Chemically Reactive Fluid Flow During Metamorphism. Annual Review of Earth and Planetary Sciences 26, 255-287.

Fourcade S., Marquer D., Javoy M., 1989. $^{18}O/^{16}O$ variations and fluid circulation in a deep shear zone-the case of the alpine ultramylonites from the aar massif central Alps, Switzerland. Chemical Geology 77, 119-131.

Fournier R.O. and Potter R.W., 1982. An equation correlating the solubility of quartz in water from 25° to 900 °C at pressures up to 10,000 bars. Geochimica et Cosmochimica Acta 46, 1969-1973.

Frey M., Bucher K., Frank E., Mullis J., 1980. Alpine metamorphism along the Geotraverse Basel-Chiasso, a review. Eclogae Geologicae Helvetiae 73, 527-546.

Frey M., Hunziker J.C., Frank W., Bocquet J., Dal Piaz G.V., Jaeger E., Niggli E., 1974. Alpine metamorphism of the Alps, a review. Schweizerische Mineralogische 54, 247-290.

Frey M., 1999. The new metamorphic map of the Alps: introduction. Schweizerische Mineralogische und Petrographische Mitteilungen, 79, 1-4.

Gasquet D., Giraud P., Ploquin A., Vivier G., 1981. Géochimie de mylonites et relations entre les Rameaux Interne et Externe du Massif de Belledonne (Alpes françaises). Comptes rendus de l'Académie des Sciences Paris, t. 292, Série II, 607-610.

Goncalves P., Oliot E., Marquer D., Connolly J.A.D., 2012. Role of chemical processes on shear zone formation: An example from the Grimsel metagranodiorite (Aar massif, Central Alps). Journal of Metamorphic Geology 30, 703-722.

Grant J., 1986. The isocon diagram-a simple solution to Gresens' equation for metasomatic alteration. Economic Geology 81, 1976-198.

Grant J.A., 2005. Isocon analysis: A brief review of the method and applications. Physics and Chemistry of the Earth 30, 997-1004.

Gresens R.L., 1967. Composition-volume relationships of metasomatism. Chemical Geology 2, 47-65.

Harlov D.E. and Austrheim H., 2013. Metasomatism and the Chemical Transformation of Rock - The Role of Fluids in Terrestrial and Extraterrestrial Processes. Lecture Notes in Earth System Sciences, Spinger, Berlin, 800 pp.

Hippertt J.F., 1998. Breakdown of feldspar, volume gain and lateral mass transfer during mylonitization of granitoid in a low metamorphic grade shear zone. Journal of Structural Geology 20, 175-193.

Holland T.J.B. and Powell R., 1985. An internally consistent thermodynamic dataset with uncertainties and correlations: 2: Data and results. Journal of Metamorphic Geology 3, 343-370.

Jones K.A. and Brown M., 1990. High-temperature "clockwise" P-T paths and melting in the development of regional migmatites: an example from Southern Brittany, France. Journal of Metamorphic Geology 14, 361-379.

Kennedy G.C., 1950. A portion of the system silica-water. Economic Geology 45, 629-653.

Labhart T.P., 1999. Aarmassiv, Gotthardmassiv und Tavetscher Zwischenmassiv: aufbau und Entstehungsgeschichte. In: Löw, S. and Wyss, R. (Eds.), Symposium Geologie Alptransit. Balkema, Rotterdam ⁄ Brookfield, Zürich, 31-43.

Le Goff E., 1989. Conditions pression-température de la déformation dans les orthogneiss: modèle thermodynamique et exemples naturels. Mémoires et documents du Centre armoricain d'étude structurale des socles, Rennes, 321 pp.

Maggi M., Rossetti F., Corfu F., Theye T., Andersen T.B., Faccenna C., 2012. Clinopyroxene-rutile phyllonites from the East Tenda Shear Zone (Alpine Corsica, France): Pressure-temperature-time constraints to the Alpine reworking of

Variscan Corsica. Journal of the Geological Society 169, 723-732.

Maggi M., Rossetti F., Ranalli G., Theye T., 2014. Feedback between fluid infiltration and rheology along a regional ductile-to-brittle shear zone: The East Tenda Shear Zone (Alpine Corsica). Tectonics 33, 253-280.

Manning C.E., 1994. The solubility of quartz in H_2O in the lower crust and upper mantle. Geochimica et Cosmochimica Acta 58, 4831-4839.

Manning, C.E., 2018. Fluids of the Lower Crust: Deep Is Different. Annual Review of Earth and Planetary Sciences 46, 67-97.

Marquer D., Gapais D., Capdevila R., 1985. Comportement chimique et orthogneissification d'une granodiorite en faciès verts (Massif de l'Aar, Alps Centrales). Bulletin de Mineralogie 108, 209-221.

Martin L.A.J., Rubatto D., Vitale Brovarone A., Hermann J., 2011. Late Eocene lawsonite-eclogite facies metasomatism of a granulite sliver associated to ophiolites in Alpine Corsica. Lithos 125, 620-640.

Mason R., 1973. The Limpopo Mobile Belt-southern Africa. Philosophical Transaction of the Royal Society of London 273, 463-485.

McCaig A.M., 1988. Deep fluid circulation in fault zones. Geology 16, 867-870.

Molli G., Tribuzio R., Marquer D., 2006. Deformation and metamorphism at the eastern border of the Tenda Massif (NE Corsica): a record of subduction and exhumation of continental crust. Journal of Structural Geology 28, 1748-1766.

Oliot E., Goncalves P., Marquer D., 2010. Role of plagioclase and reaction softening in a metagranite shear zone at mid-crustal conditions (Gotthard Massif, Swiss Central Alps). Journal of Metamorphic Geology 28, 849-871.

Ord A. and Oliver N.H.S., 1997. Mechanical controls on fluid flow during regional metamorphism: Some numerical models. Journal of Metamorphic Geology 15, 345-359.

Pili E., Sheppard S.M.F., Lardeaux J.M., 1999. Fluid-rock interaction in the granulites of Madagascar and lithospheric transfer of fluids. Gondwana Research 2, 341-350.

Powell R. and Holland T.J.B., 1988. An internally consistent thermodynamic dataset with uncertainties and correlations: 3. Application, methods, worked examples and a computer program. Journal of Metamorphic Geology 6, 173-204.

Raimondo T., Clark C., Hand M., Faure K., 2011. Assessing the geochemical and tectonic impacts of fluid-rock interaction in mid-crustal shear zones: A case study from the intracontinental Alice Springs Orogen, central Australia. Journal of Metamorphic Geology 29, 821-850.

Roering C., van Reenen D.D., Smit C.A., Barton J.M., de Beer J.H., de Wit M.J., Stettler E.H., van Schalkwyk J.F., Stevens G., Pretorius S., 1992. Tectonic model for the evolution of the Limpopo Belt. Precambrian Research 55, 539-552.

Rolland Y. and Rossi M., 2016. Two-stage fluid flow and element transfers in shear zones during collision burial-exhumation cycle: Insights from the Mont Blanc Crystalline Massif (Western Alps). Journal of Geodynamics 101, 88-108.

Rolland Y., Cox S., Boullier A.M., Pennacchioni G., Mancktelow N., 2003. Rare earth and trace element mobility in mid-crustal shear zones: Insights from the Mont Blanc Massif (Western Alps). Earth and Planetary Science Letters 214, 203-219.

Rolland Y., Cox S.F., Corsini M., 2009. Constraining deformation stages in brittle-ductile shear zones from combined field mapping and $^{40}Ar/^{39}Ar$ dating: The structural evolution of the Grimsel Pass area (Aar Massif, Swiss Alps). Journal of Structural Geology 31, 1377-1394.

Rolland Y., Rossi M., Cox S.F., Corsini M., Mancktelow N., Pennacchioni G., Fornari M., Boullier A.M., 2008. $^{40}Ar/^{39}Ar$ dating of synkinematic white mica: insights from fluid-rock reaction in low-grade shear zones (Mont Blanc Massif) and constraints on timing of deformation in the NW external Alps. Geological Society, London, Special Publications 299, 293-315.

Rossi M. and Rolland Y., 2014. Stable isotope and Ar/Ar evidence of prolonged multiscale fluid flow during exhumation of orogenic crust: Example from the mont blanc and Aar Massifs (NW Alps). Tectonics 33, 1681-1709.

Rossi M., Rolland Y., Vidal O., Cox S.F., 2005. Geochemical variations and element transfer during shear-zone development and related episyenites at middle crust depths: insights from the Mont Blanc granite (French-Italian Alps). Geological Society, London, Special Publications 245, 373-396.

Rumble D., Liou J.G., Jahn B.M., 2003. Continental crust subduction and ultrahigh pressure metamorphism. In: Treatise on Geochemistry. (Eds.): H.D. Holland and K.K. Turekian. Elsevier Science, 293-319.

Sanchez G., Rolland Y., Schneider J., Corsini M., Oliot E., Goncalves P., Verati C., Lardeaux J.-M., Marquer D., 2011. Dating low-temperature deformation by $^{40}Ar/^{39}Ar$ on white mica, insights from the Argentera-Mercantour Massif (SW Alps) Lithos 125, 521-536.

Sassier C., Boulvais P., Gaspais D., Capdevila R., Diot H., 2006. From granitoid to kyanite-bearing micaschist during fluid-assisted shearing (Ile d'Yeu, France). International Journal of Earth Sciences 95, 2-18.

Schulien S., 1980. Mg-Fe partitioning between biotite and a supercritical chloride solution. Contributions to Mineralogy and Petrology 74, 85-93.

Selverstone J., Morteani G., Staude J.-M., 1991. Fluid channelling during ductile shearing: transformation of granodiorite into aluminous schist in the Tauern Window, Eastern Alps. Journal of Metamorphic Geology 9, 419-431.

Semelin B. and Marchand J., 1984. Découverte d'enclaves hyper-alumineuses dans l'ortho-gneiss de l'Ile d'Yeu. Comptes rendus de l'Académie des Sciences Paris, série II, 299, 633-638.

Shmulovich K.I., Yardley B.W.D., Graham C.M., 2006. Solubility of quartz in crustal fluids: Experiments and general equations for salt solutions and H_2O-CO_2 mixtures at 400-800 °C and 0.1-0.9 GPa. Geofluids 6, 154-167.

Spear F.S. and Menard T., 1989. Program GIBBS: A generalized Gibbs method algorithm. American Mineralogist 74, 942-943.

Steck A., 1976. Albit-Oligoklas-Mineralgesellschaften der Peristeritlücke aus alpinmetamorphen Granitgneisen des Gotthardmassivs Schweizerische Mineralogische und Petrographische Mitteilungen 56, 269-292.

Streit J.E. and Cox S.F., 1998. Fluid infiltration and volume change during mid-crustal mylonitization of Proterozoic granite, King Island, Tasmania. Journal of Metamorphic Geology 16, 197-212.

Streit J.E., 1994. Effects of fluid-rock interaction on shear zone evolution in Proterozoic granites on King Island, Tasmania. Ph.D. thesis, The Australian National University, Camberra.

Tobisch O.T., Barton M.D., Vernon R.H., Paterson S.R., 1991. Fluid-Enhanced Deformation : Transformation of Granitoids to Banded Mylonites, Wester Sierra Nevada, California, and Outheastern Austrailia. Journal of Structural Geology 13, 1137-1156.

Tsunogae T. and van Reenen D.D., 2014. High- to ultrahigh-temperature metasomatism related to brine infiltration in the Neoarchean Limpopo Complex: Petrology and phase equilibrium modeling. Precambrian Research 253, 157-170.

Van Reenen D.D., Barton J.M., Roering C., Smith C.A., Van Schalkwyk J.F., 1987. Deep crustal response to continental collision: the Limpopo belt of southern Africa. Geology 15, 11-14.

van Staal C.R., Ravenhurst C., Winchester J., Roddick J., Langton J., 1990. Post-Tectonic blueschist suture in the northern Appalachians of northern New Brunswick, Canada. Geology 18, 1073-1077.

van Staal C.R., Rogers N., Taylor B.E., 2001. Formation of low-temperature mylonites and phyllonites by alkali-metasomatic weakening of felsic volcanic rocks during progressive, subduction-related deformation. Journal of Structural Geology 23, 903-921.

Vitale Brovarone A., Beyssac O., Malavieille J., Molli G., Beltrando M., Compagnoni R., 2013. Stacking and metamorphism of continuous segments of subducted lithosphere in a high-pressure wedge: The example of Alpine Corsica (France). Earth-Science Reviews 116, 35-36.

Walther J.V. and Helgeson H.C., 1977. Calculation of the thermodynamic properties of aqueous silica and the solubility of quartz and its polymorphs at high pressures andtemperatures. American Journal of Science 277, 1315-1351.

Walther J.V. and Orville P.M., 1983. The extraction-quench technique for determination of the thermodynamic properties of solute complexes: application to quartz solubility in fluid mixtures. American Mineralogist 68, 731-41.

Whitney D.L. and Evans B.W., 2010. Abbreviations for names of rock-forming minerals. American Mineralogist 95, 185-187. doi:10.2138/am.2010.3371.

Winter J.D., 2014. Principles of Igneous and Metamorphic Petrology. Pearson New International Edition, 738 pp.

Wintsch R.P., Christoffersen R., Kronenberg A.K., 1995. Fluid-rock reaction weakening of fault zones. Journal of Geophysical Research 100, 13021-13032.

Wood B.J. and Walther J.V., 1986. Fluid flow during metamorphism and its implications for fluid-rock ratios. In: Fluid-rock Interaction During Metamorphism. (Eds.): J.V. Walther and B.J. Wood. Springer, Berlin, 89-109.